

## Article

# Locking Phenomena in Semiconductor Lasers Near Threshold with Optical Feedback and Sinusoidal Current Modulation

Jordi Tiana-Alsina <sup>1</sup>  and Cristina Masoller <sup>2,\*</sup> 

<sup>1</sup> Department de Física Aplicada, Facultat de Física, Universitat de Barcelona, Martí i Franquès 1, 08028 Barcelona, Spain; jordi.tiana@ub.edu

<sup>2</sup> Departament de Física, Universitat Politècnica de Catalunya, Rambla Sant Nebridi 22, 08222 Terrassa, Spain

\* Correspondence: cristina.masoller@upc.edu

**Abstract:** The dynamics of semiconductor lasers with optical feedback and current modulation has been extensively studied, and it is, by now, well known that the interplay of modulation and feedback can produce a rich variety of nonlinear phenomena. Near threshold, in the so-called low frequency fluctuations regime, the intensity emitted by the laser, without modulation, exhibits feedback-induced spikes, which occur at irregular times. When the laser current is sinusoidally modulated, under appropriate conditions, the spikes lock to the modulation and become periodic. In previous works, we studied experimentally the locked behavior and found sub-harmonic locking (regular spike timing such that a spike is emitted every two or three modulation cycles), but we did not find spikes with regular timing, emitted every modulation cycle. To understand why 1:1 regular locking was not observed, here, we perform simulations of the well-known Lang–Kobayashi model. We find a good qualitative agreement with the experiments: with small modulation amplitudes, we find wide parameter regions in which the spikes are sub-harmonically locked to the modulation, while 1:1 locking occurs at much higher modulation amplitudes.

**Keywords:** semiconductor lasers; diode lasers; optical feedback; modulation; locking; laser dynamics; nonlinear dynamics



**Citation:** Tiana-Alsina, J.; Masoller, C. Locking Phenomena in Semiconductor Lasers Near Threshold with Optical Feedback and Sinusoidal Current Modulation. *Appl. Sci.* **2021**, *11*, 7871. <https://doi.org/10.3390/app11177871>

Academic Editors: Wolfgang Elsaesser and Frédéric Grillot

Received: 17 June 2021

Accepted: 18 August 2021

Published: 26 August 2021

**Publisher's Note:** MDPI stays neutral with regard to jurisdictional claims in published maps and institutional affiliations.



**Copyright:** © 2021 by the authors. Licensee MDPI, Basel, Switzerland. This article is an open access article distributed under the terms and conditions of the Creative Commons Attribution (CC BY) license (<https://creativecommons.org/licenses/by/4.0/>).

## 1. Introduction

Semiconductor lasers with optical feedback provide an experimental testbed to study a rich variety of nonlinear phenomena. While the free-running laser is a two-dimensional system that displays only transient relaxation oscillations, the feedback delay time expands the dimensionality of the system, and induces multistability of stable solutions (the so-called external cavity modes) and sustained periodic or chaotic oscillations [1–3]. A small-amplitude periodic modulation of the laser current can control feedback-induced oscillations, but it can also generate bistability, for example, of small and large chaotic oscillations [4].

Near the threshold, a regime known as low-frequency fluctuations occurs in which the laser intensity abruptly drops to zero and recovers gradually. In the absence of current modulation, the intensity dropouts (which we will refer to as spikes) occur at irregular times. With modulation, under appropriate conditions, they can lock to the modulation, and a spike is emitted every  $n$  modulation cycles [5–17].

The laser dynamics with optical feedback and current modulation is interesting because it has three time scales that can be controlled experimentally: the “natural”, unmodulated spike rate (controlled by the DC value of the laser pump current and the feedback conditions [18]), the external cavity frequency (controlled by the length of the feedback cavity) and the modulation frequency. By tuning these parameters, different locked and unlocked behaviors can occur. We have studied the locking regimes, by performing experiments with different lasers, feedback conditions and modulation waveforms [19–21]. We have found that small-amplitude sinusoidal current modulation can generate rigid and

regular subharmonically locked spikes: rigid in the sense that the locked behavior persists in a parameter region, and regular in the sense that the spike timing is regular over very long time intervals [21]. However, we did not find rigid and regular harmonic locking. In this paper, we aim to shed light into the elusiveness of the regular 1:1 locked spikes.

This paper is organized as follows. In Section 2, we present the model used to simulate the dynamics of the laser. In Section 3, we present the results of the simulations, and in Section 4, we present the discussion and the conclusions.

## 2. Model

The Lang–Kobayashi rate equations [1] describing a single-mode semiconductor laser with optical feedback and sinusoidal pump current modulation, in simplified notation [22,23], are as follows:

$$\dot{E} = k(1 + i\alpha)(G - 1)E + \eta E(t - \tau)e^{-i\omega_0\tau} + \sqrt{D}\xi, \quad (1)$$

$$\dot{N} = \gamma_N(\mu_{dc} + a_{mod} \sin(2\pi f_{mod}t) - N - G|E|^2). \quad (2)$$

In these equations,  $E$  represents the slowly varying complex optical field ( $|E|^2$  is proportional to the laser intensity) and  $N$  represents the carrier density.  $\eta$ ,  $\tau$ , and  $\omega_0\tau$  are the feedback strength, the delay time and the feedback phase, respectively;  $k = 1/(2\tau_p)$  where  $\tau_p$  is the photon lifetime,  $\gamma_N = 1/\tau_N$  where  $\tau_N$  is the carrier lifetime,  $G = N/(1 + \epsilon|E|^2)$  is the gain and  $\epsilon$  is the gain saturation coefficient,  $\alpha$  is the linewidth enhancement factor.  $\mu_{dc}$ ,  $a_{mod}$  and  $f_{mod}$  are the  $dc$  value, the amplitude and the frequency of the sinusoidal modulation of the pump current, respectively.

Spontaneous emission noise is taken into account by a complex additive Gaussian white noise,  $\xi$ , with strength  $D$ . In the deterministic model ( $D = 0$ ), for typical parameters, the spikes are a transient dynamics, after which the laser output is stable (the laser emits the stable external cavity mode that has maximum gain). With large enough noise, the spiking dynamics can become stable, sustained by noise [24,25]. Therefore, in this model, the spikes are generated by the interplay of deterministic and stochastic mechanisms. The coexistence of stable emission and spiking behavior was reported in Ref. [26]. While this model explains many observations, it has several simplifications: it assumes single-mode emission, it considers a single reflection in the external cavity, and it neglects spatial inhomogeneities in the optical field and in the carrier population.

## 3. Results

The model equations were integrated with the following (typical) parameters that fit the experimental conditions in [19–21]:  $k = 300 \text{ ns}^{-1}$ ,  $\gamma_N = 1 \text{ ns}^{-1}$ ,  $\alpha = 4$ ,  $\epsilon = 0.01$ ,  $\eta = 30 \text{ ns}^{-1}$ ,  $\tau = 5 \text{ ns}$ ,  $\mu_{dc} = 0.99$  and  $D = 10^{-5} \text{ ns}^{-2}$ . The Euler–Maruyama method with an integration step of  $dt = 1 \text{ ps}$  was used to integrate the equations. The initial conditions were chosen with the laser off and after disregarding a transient time of  $50 \mu\text{s}$ , the equations were integrated for  $10 \mu\text{s}$ . To detect the spike times the intensity time series,  $|E(t)|^2$  was band-pass filtered [27] to simulate the finite bandwidth of the experimental detection system, and was normalized to zero mean and unit variance. Then, a spike was detected when the intensity decreased below the threshold  $Th = -1.1$ .

In Figure 1, we analyze the statistics of the spike sequences, as a function of the modulation amplitude and frequency. Figure 1 displays in color code the number of spikes in the intensity time series (panel a), the mean inter-spike-interval (ISI) normalized to the modulation period (panel b), and the normalized standard deviation of the ISI distribution (panel c,  $\sigma_{ISI}/\langle ISI \rangle$ , in logarithmic scale). In panel (a), we see that the spikes become more frequent with increasing  $a_{mod}$  and  $f_{mod}$ , i.e., the spikes become faster with  $a_{mod}$  and  $f_{mod}$ . In panel (b) we can differentiate five regions: in blue,  $\langle ISI \rangle/T_{mod} \approx 1$ , in cyan,  $\langle ISI \rangle/T_{mod} \approx 2$ , in green,  $\langle ISI \rangle/T_{mod} \approx 3$ , in yellow  $\langle ISI \rangle/T_{mod} \approx 4$ , and in red  $\langle ISI \rangle/T_{mod} \geq 5$ . We do not find 5:1 locking, and we interpret that this is likely due to the fact that the 5:1 locking region would be located at high modulation frequencies, where the spikes are poorly defined, as the intensity displays quite chaotic fluctuations.

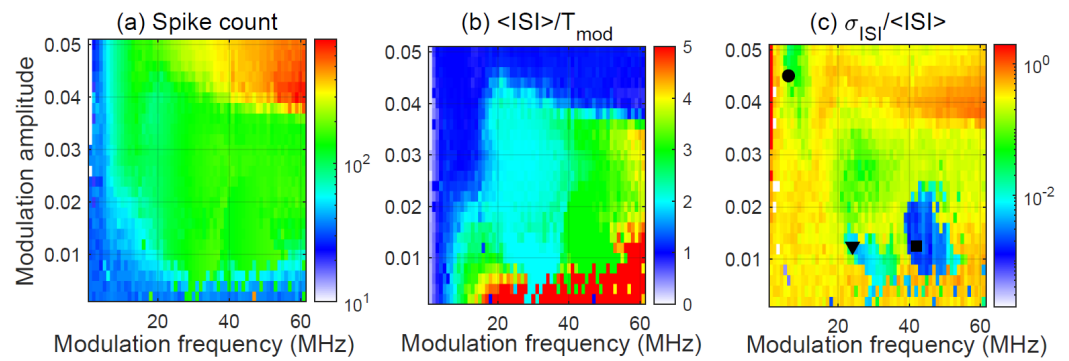


**Figure 1.** (a) Number of spikes in the intensity time series, in logarithmic color code, as a function of the modulation amplitude and frequency. (b) Mean inter–spike–interval, normalized to the period of the modulation. Here, the color scale is saturated such that red represents  $\langle ISI \rangle / T_{mod} \geq 5$ . (c) Standard deviation of the ISI distribution normalized to the mean ISI. Note the logarithmic color scale. The symbols indicate the parameters used in Figure 2.

To determine where, within these regions, the spikes are regularly locked to the sinusoidal modulation, we need to inspect panel (c), where very low values of  $\sigma_{ISI} / \langle ISI \rangle$  ( $< 10^{-2}$ , blue regions) reveal a narrow ISI distribution (i.e., a regular spike timing). In panel (c), we see two well-defined blue regions (light blue and dark blue). In these regions, in panel (b) we see that  $\langle ISI \rangle / T_{mod} = 2$  or 3. Comparing panels (b) and (c), we see that for the blue regions in panel (b) [ $\langle ISI \rangle / T_{mod} \approx 1$ ],  $\sigma_{ISI} / \langle ISI \rangle > 10^{-2}$  in panel (c); therefore, the timing of the spikes when  $\langle ISI \rangle \approx T_{mod}$  is significantly more irregular than the timing of 2:1 and 3:1 locked spikes.

Examples of the intensity time series in the different locking regions are presented in Figure 2. The shape of the oscillations after each spike is similar for 2:1 and 3:1 locking, but it is very different for 1:1 locking, as in this case the spike is of very small amplitude. For 2:1 and 3:1 locking (panels b and c), in our previous works, we have reported very similar experimental time series (see Figure 1 in [20]). In our previous works, the modulation was of a small amplitude and we did not observe 1:1 locking of the form shown in Figure 2a. However, a very similar experimental time series of 1:1 locked spikes was reported in Ref. [8] (Figure 3f, which is for a modulation amplitude of 13.8% of the DC level of the laser current).

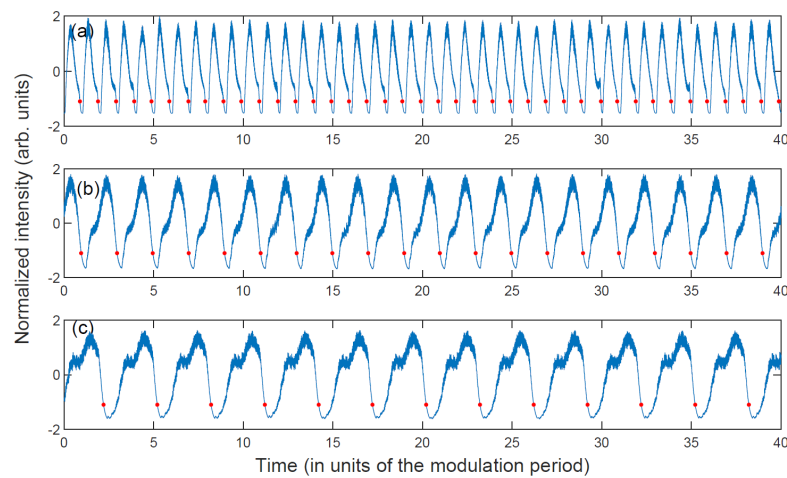


**Figure 2.** Time series of the laser intensity (normalized to zero–mean and unit variance) in different locking regions: (a) 1:1 locking for  $f_{mod} = 5$  MHz,  $a_{mod} = 0.045$ ; (b) 2:1 locking for  $f_{mod} = 24$  MHz,  $a_{mod} = 0.0125$ ; (c) 3:1 locking for  $f_{mod} = 42$  MHz,  $a_{mod} = 0.0125$  (these parameters were indicated in Figure 1 with a circle, a triangle, and a square, respectively). In all panels, the red dots mark the spike times (when the intensity decreases below the threshold  $-1.1$ ).

To unveil the role of the modulation amplitude, we show in Figures 3 and 4 the effect of increasing  $a_{mod}$ , for two modulation frequencies such that for appropriate  $a_{mod}$ , the modulation produces 1:1 (Figure 3) or 2:1 (Figure 4) locked spikes. In Figure 3, we see that 1:1 locking occurs for high enough  $a_{mod}$  (panel e), while if the modulation amplitude is not too large (as in our experiments), we see that the spike timing is irregular. Note that in this figure, panel (a) displays the “natural”, unmodulated intensity dynamics. In Figure 4 we see that regular 2:1 locking occurs for  $a_{mod} = 0.0125$  [panel (b)]. The locked behavior is rigid in the sense that it persists in a range of  $a_{mod}$  values; if  $a_{mod}$  is too small, the spike timing is irregular, while if it is too large, the spikes become poorly defined. The locking region has smooth boundaries; therefore, we cannot define a precise range of  $a_{mod}$  values. However, we can see that in panels (a) and (d) the spikes are not locked, while in panels (b) and (c), they are locked.

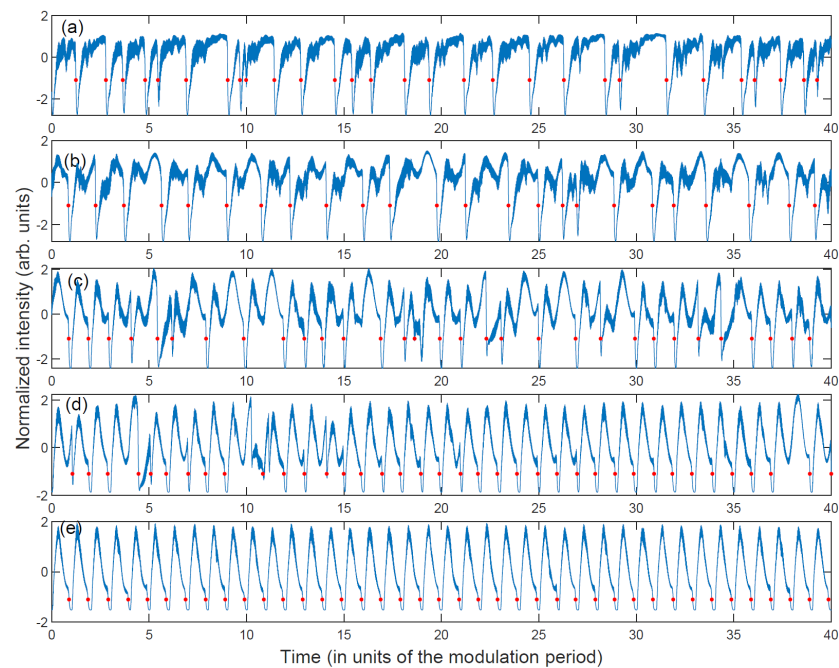


**Figure 3.** Intensity time series for increasing modulation amplitude:  $a_{mod} = 0$  (a), 0.01 (b), 0.025 (c), 0.04 (d), 0.05 (e).  $f_{mod} = 5$  MHz; other parameters are as indicated in the text.

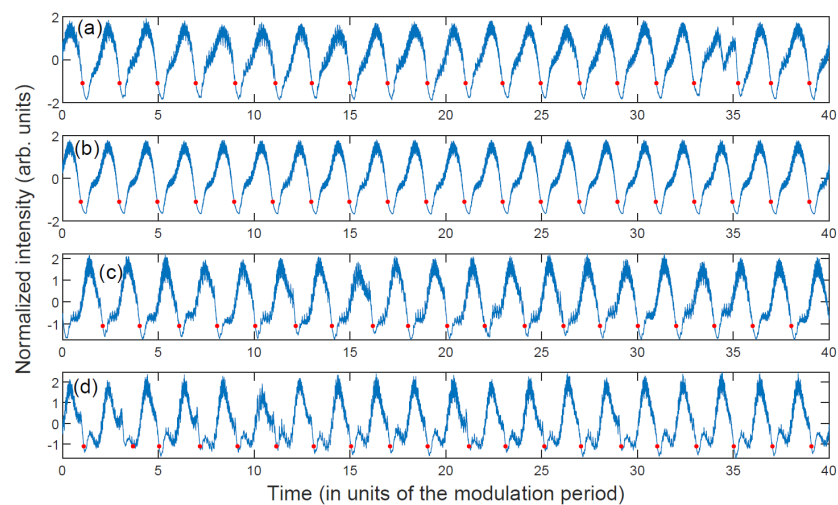


**Figure 4.** Intensity time series for  $a_{mod} = 0.01$  (a), 0.0125 (b), 0.02 (c), 0.03 (d).  $f_{mod} = 24$  MHz; other parameters are as indicated in the text.

The locking regions are separated by regions where the spikes are unlocked. An example of the transition of 2:1 locking to 3:1 locking that occurs when the modulation frequency increases is shown in Figure 5. This transition corresponds to moving along an horizontal line in the panels displayed in Figure 1. In Figure 5 we see that for  $f_{mod} = 35$  MHz (panel a) and 40 MHz (panel d), the spikes are locked (2:1 and 3:1, respectively) while for frequencies in between, there is the intermittent alternation of 2:1 and 3:1 locked spikes. This is consistent with the results shown in Figure 1c, where we see that  $\sigma_{ISI}/\langle ISI \rangle$  is small in the locking regions, while it grows in the transition region.

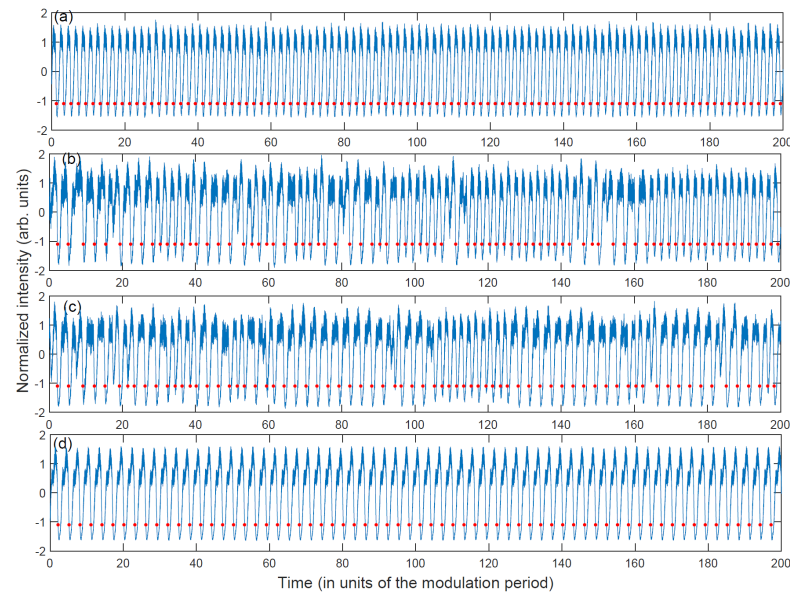


**Figure 5.** Transition between 2:1 and 3:1 regular locking, when the modulation frequency increases while the modulation amplitude is kept constant. The parameters are  $a_{mod} = 0.0125$  and  $f_{mod} = 35$  MHz (a), 37 MHz (b), 39 MHz (c), 40 MHz (d).

For particular values of the modulation amplitude and frequency, a spike can occur every modulation cycle. An example is shown in Figure 6a; it corresponds, in Figure 1b to the “blue dot” within the green area. There is no “rigid” locking as the regular spiking dynamics is not robust to small changes of the parameters (i.e., there is no range of frequencies or amplitudes within which the regular behavior persists). We note that the shape of the spikes in Figure 6a and in Figure 2a is different. This may be due to the fact that the modulation parameters, both amplitude and frequency, are very different: in Figure 6a,  $a_{mod} = 0.012$ ,  $f_{mod} = 16$  MHz, while in Figure 2a,  $a_{mod} = 0.045$ ,  $f_{mod} = 5$  MHz. This “blue dot” is visible because it is located within the green area; it is possible that other “blue dots” exist that are not visible because they are located within the blue area.

As explained before, optical feedback introduces a set of coexisting steady-state solutions (the external cavity modes, ECMs, which can be stable modes or unstable modes). Under current modulation the ECMs turn into limit cycles that can be stable or unstable. For particular values of the modulation amplitude and frequency, after a transient, the system ends in a limit cycle and the intensity displays periodic oscillations without spikes. An example is shown in Figure 6b. When this occurs, after the transient,  $\langle ISI \rangle / T_{mod} = 1$  and  $\sigma_{ISI} / \langle ISI \rangle$  is small. As in the case of 1:1 locked spikes, there is no “rigidity”, i.e., we have not found parameter regions where these regular oscillations persist. Therefore, in Figure 1b,c, in the blue dots where  $\langle ISI \rangle / T_{mod} = 1$  and  $\sigma_{ISI} / \langle ISI \rangle$  is small, the intensity can display 1:1 locked spikes, or periodic oscillations without spikes.

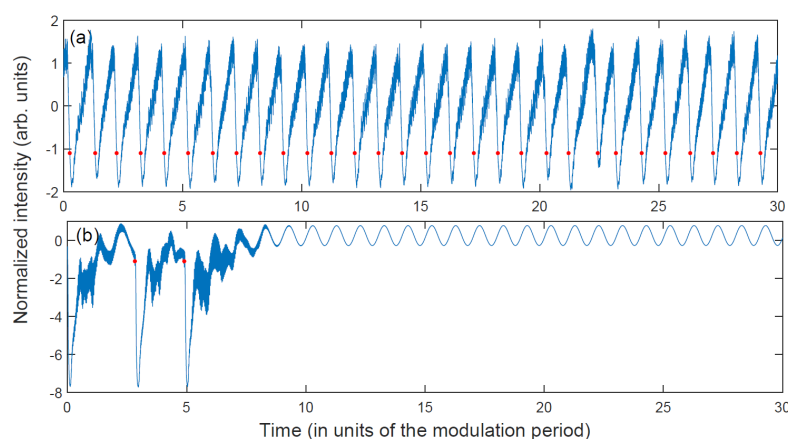


**Figure 6.** Intensity time series displaying (a) 1:1 locked spikes ( $f_{mod} = 16$  MHz,  $a_{mod} = 0.012$ ); (b) transient spiking dynamics followed by periodic oscillations ( $f_{mod} = 6$  MHz,  $a_{mod} = 0.006$ ).

These results are robust with respect to small changes of the DC level of the laser current. We remark that the low frequency fluctuation regime (where the intensity displays well-defined spikes), occurs near the solitary threshold, in a limited range of pump current values: if we decrease or increase too much  $\mu_{dc}$  the spikes become not well defined, either because the intensity fluctuations are too noisy, or because they are too fast and chaotic [28,29].

#### 4. Discussion

To summarize, we have studied numerically the dynamics of a semiconductor laser with optical feedback and sinusoidal current modulation. We simulated the Lang–Kobayashi model to understand why, with small-amplitude modulation, regular 1:1 locked spikes was not observed experimentally. The simulations have allowed us to identify the locking regions in the parameter space (modulation amplitude, modulation frequency). We have found subharmonically locked spikes (2:1 and 3:1) when the modulation is fast enough, and its amplitude is not too large. We have also found 1:1 locked spikes that occur at a higher modulation amplitude and lower modulation frequency, but in this case, the spike timing is more irregular (for subharmonic locking, the normalized standard deviation is  $<10^{-2}$ , while for harmonic locking, it is  $>10^{-2}$ ).

Our interpretation of the physical mechanisms behind these results is the interplay of the laser dynamics near the threshold and the modulation-induced dynamics. While locking phenomena in nonlinear oscillators is well understood and broadly applied, in laser systems, the existence of the threshold introduces additional nonlinear behaviors not observed in conventional, threshold-less oscillators. In the situation considered here, because the laser is near the threshold (where the feedback-induced spiking dynamics occurs), in each modulation cycle, the pump current brings the laser close or below the threshold, and at low modulation frequencies, this occurs for a duration long enough to prevent the generation of fully regular 1:1 locked behavior (due to fluctuations in the timing of the turn-on pulses—the so-called timing jitter). However, when the modulation frequency increases, the intervals during which the pump current is close or below the threshold are shorter, and the current modulation can generate regular 2:1 and 3:1 locked behaviors. It will be interesting, for future work, to analyze how the optical feedback parameters affect the spike timing regularity.

**Author Contributions:** Conceptualization, methodology, analysis, and writing, J.T.-A. and C.M. All authors have read and agreed to the published version of the manuscript.

**Funding:** This research was funded by the Spanish Ministerio de Ciencia, Innovacion y Universidades (PGC2018-099443-B-I00) and the ICREA ACADEMIA program of Generalitat de Catalunya.

**Institutional Review Board Statement:** Not applicable.

**Informed Consent Statement:** Not applicable.

**Data Availability Statement:** Not applicable.

**Conflicts of Interest:** The authors declare no conflict of interest.

## References

1. Lang, R.; Kobayashi, K. External optical feedback effects on semiconductor injection-laser properties. *IEEE J. Quantum Electron.* **1980**, *16*, 347. [[CrossRef](#)]
2. Lenstra, D.; Verbeek, B.H.; Denboef, A.J. Coherence collapse in single-mode semiconductor-lasers due to optical feedback. *IEEE J. Quantum Electron.* **1985**, *21*, 674. [[CrossRef](#)]
3. Mork, J.; Tromborg, B.; Mark, J. Chaos in semiconductor-lasers with optical feedback: Theory and experiment. *IEEE J. Quantum Electron.* **1992**, *28*, 93. [[CrossRef](#)]
4. Ohtsubo, J. *Semiconductor Lasers: Stability, Instability and Chaos*, 4th ed.; Springer: Berlin, Germany, 2017.
5. Baums, D.; Elsasser, W.; Gobel, E.O. Farey tree and Devil's staircase of a modulated external-cavity semiconductor laser. *Phys. Rev. Lett.* **1989**, *63*, 155. [[CrossRef](#)]
6. Sacher, S.; Baums, D.; Panknin, P.; Elsasser, W.; Gobel, E.O. Intensity instabilities of semiconductor-lasers under current modulation, external light injection, and delayed feedback. *Phys. Rev. A* **1992**, *45*, 1893. [[CrossRef](#)] [[PubMed](#)]
7. Takiguchi, Y.; Liu, Y.; Ohtsubo, J. Low-frequency fluctuation induced by injection-current modulation in semiconductor lasers with optical feedback. *Opt. Lett.* **1998**, *23*, 1369. [[CrossRef](#)]
8. Sukow, D.W.; Gauthier, D.J. Entraining power-dropout events in an external-cavity semiconductor laser using weak modulation of the injection current. *IEEE J. Quantum Electron.* **2000**, *36*, 175. [[CrossRef](#)]
9. Mendez, J.M.; Laje, R.; Giudici, M.; Aliaga, J.; Mindlin, G.B. Dynamics of periodically forced semiconductor laser with optical feedback. *Phys. Rev. E* **2001**, *63*, 066218. [[CrossRef](#)]
10. Lawrence J.S.; Kane, D.M. Nonlinear dynamics of a laser diode with optical feedback systems subject to modulation. *IEEE J. Quantum Electron.* **2002**, *38*, 185. [[CrossRef](#)]
11. Marino, F.; Giudici, M.; Barland, S.; Balle, S. Experimental evidence of stochastic resonance in an excitable optical system. *Phys. Rev. Lett.* **2002**, *88*, 040601. [[CrossRef](#)] [[PubMed](#)]
12. Lam, W.-S.; Guzdar, P. N.; Roy, R. Effect of spontaneous emission noise and modulation on semiconductor lasers near threshold with optical feedback. *Int. J. Mod. Phys. B* **2003**, *17*, 4123. [[CrossRef](#)]
13. Torre, M. S.; Masoller, C.; Mandel, P.; Shore K.A. Transverse-mode dynamics in directly modulated vertical-cavity surface-emitting lasers with optical feedback. *IEEE J. Quantum Electron.* **2004**, *40*, 620. [[CrossRef](#)]
14. Toomey, J.P.; Kane, D.M.; Lee, M.W.; Shore, K.A. Nonlinear dynamics of semiconductor lasers with feedback and modulation. *Opt. Express* **2010**, *18*, 16955. [[CrossRef](#)] [[PubMed](#)]
15. Ahmed, M.; El-Sayed, N.Z.; Ibrahim, H. Chaos and noise control by current modulation in semiconductor lasers subject to optical feedback. *Eur. Phys. J. D* **2012**, *66*, 141. [[CrossRef](#)]
16. Spitz, O.; Wu, J.G.; Carras, M.; Wong, C.W.; Grillot, F. Chaotic optical power dropouts driven by low frequency bias forcing in a mid-infrared quantum cascade laser. *Sci. Rep.* **2019**, *9*, 4451. [[CrossRef](#)] [[PubMed](#)]
17. Spitz, O.; Wu, J.G.; Herdt, A.; Carras, M.; Elsasser, W.; Wong, C.W.; Grillot, F. Investigation of chaotic and spiking dynamics in mid-infrared quantum cascade lasers operating continuous-waves and under current modulation. *IEEE J. Sel. Top. Quantum Electron.* **2019**, *25*, 1200311. [[CrossRef](#)]
18. Hong, Y.; Shore, K.A. Statistical measures of the power dropout ratio in semiconductor lasers subject to optical feedback. *Opt. Lett.* **2005**, *30*, 3332. [[CrossRef](#)]
19. Aragonese, A.; Sorrentino, T.; Perrone, S.; Gauthier, D.J.; Torrent, M.C.; Masoller, C. Experimental and numerical study of the symbolic dynamics of a modulated external-cavity semiconductor laser. *Opt. Express* **2014**, *22*, 4705. [[CrossRef](#)]
20. Sorrentino, T.; Quintero-Quiroz, C.; Aragonese, A.; Torrent, M.C.; Masoller, C. Effects of periodic forcing on the temporally correlated spikes of a semiconductor laser with feedback. *Opt. Express* **2015**, *23*, 5571. [[CrossRef](#)]
21. Tiana-Alsina, J.; Quintero-Quiroz, C.; Panozzo, M.; Torrent, M.C.; Masoller, C. Experimental study of modulation waveforms for entraining the spikes emitted by a semiconductor laser with optical feedback. *Opt. Express* **2018**, *26*, 9298. [[CrossRef](#)]
22. Torre, M.S.; Masoller, C.; Abraham, N.B.; Ranea-Sandoval, H.F. Carrier dynamics in semiconductor lasers operating in the low-frequency fluctuation regime. *J. Opt. B Quantum Semiclass. Opt.* **2000**, *2*, 563. [[CrossRef](#)]
23. Barland, S.; Spinicelli, P.; Giacomelli, G.; Marin, F. Measurement of the working parameters of an air-post vertical-cavity surface-emitting laser. *IEEE J. Quantum Electron.* **2005**, *41*, 1235. [[CrossRef](#)]
24. Torcini, A.; Barland, S.; Giacomelli, G.; Marin, F. Low-frequency fluctuations in vertical cavity lasers: Experiments versus Lang-Kobayashi dynamics. *Phys. Rev. A* **2006**, *74*, 063801. [[CrossRef](#)]
25. Zamora-Munt, J.; Masoller, C.; Garcia-Ojalvo, J. Transient low-frequency fluctuations in semiconductor lasers with optical feedback. *Phys. Rev. A* **2010**, *81*, 033820. [[CrossRef](#)]
26. Heil, T.; Fischer, I.; Elsasser, W. Coexistence of low-frequency fluctuations and stable emission on a single high-gain mode in semiconductor lasers with external optical feedback. *Phys. Rev. A* **1998**, *58*, R2672. [[CrossRef](#)]

27. Press, W.H.; Teukolsky, S.A.; Vetterling, W.T.; Flannery, B.P. *Numerical Recipes*, 2nd ed.; Cambridge University Press: Cambridge, UK, 1992.
28. Panozzo, M.; Quintero-Quiroz, C.; Tiana-Alsina, J.; Torrent, M.C.; Masoller, C. Experimental characterization of the transition to coherence collapse in a semiconductor laser with optical feedback. *Chaos* **2017**, *27*, 114315. [[CrossRef](#)] [[PubMed](#)]
29. A Video of the Experimental Intensity Time Series, without Current Modulation, Can Be Seen Here: Noisy Fluctuations Gradually Become Well-Defined Spikes, Which Become Faster and Less Pronounced as the Pump Current Increases. Available online: [https://youtu.be/nltBQG\\_IIWQ](https://youtu.be/nltBQG_IIWQ) (accessed on 17 June 2021).